Geophysical Research Letters

RESEARCH LETTER
10.1029/2022GL099443

Key Points:

- Global climate models do not agree on the sign of 21st century precipitation trends for the southwestern United States
- Future precipitation trends in this region are closely tied to the models' present-day mid-tropospheric flow over western North America
- Models with the most biased present-day mid-tropospheric flow project the largest drying trends in winter and wetting trends in summer

Supporting Information:

Supporting Information may be found in the online version of this article.

Correspondence to:

K. M. Grise,
kmg3r@virginia.edu

Citation:

Grise, K. M. (2022). Atmospheric circulation constraints on 21st century seasonal precipitation storylines for the southwestern United States. *Geophysical Research Letters*, *49*, e2022GL099443. https://doi.org/10.1029/2022GL099443

Received 11 MAY 2022
Accepted 20 AUG 2022

Atmospheric Circulation Constraints on 21st Century Seasonal Precipitation Storylines for the Southwestern United States

Kevin M. Grise[1]

[1]Department of Environmental Sciences, University of Virginia, Charlottesville, VA, USA

Abstract Precipitation is vital for the water-limited region of the southwestern United States. Coupled Model Intercomparison Project Phase 6 global climate models project 21st century precipitation trends of varying sign for this region, even if forced by an identical anthropogenic emissions scenario. This study investigates the role of the present-day and future atmospheric circulation in driving the disparity in precipitation trends among models. The wettest model projections are linked to the development of an anomalous mid-tropospheric trough over the eastern North Pacific Ocean, which depends in part on future unpredictable internal variability. By contrast, future precipitation trends are also linked to models' representation of the present-day climatological mid-tropospheric ridge over western North America. Models that fail to properly simulate this ridge in the present-day climatology are responsible for the most extreme outlier precipitation scenarios for the Southwest for the 21st century: extreme drying in winter and extreme wetting in summer.

Plain Language Summary The southwestern United States contains major population centers and agricultural regions that depend on limited water resources. Computer models used to predict future climate change disagree on how precipitation will change in this region over the 21st century. The goal of this study is to investigate why different models predict different future precipitation changes for this region. The key finding is that how well models simulate the present-day configuration of the atmospheric jet streams over western North America is closely linked to what they predict for future precipitation change in the Southwest. By excluding models with poor representations of the present-day jet streams, the range of physically plausible future precipitation scenarios for the Southwest can be narrowed to exclude extreme drying trends during winter and extreme wetting trends during summer.

1. Introduction

The southwestern United States ("the Southwest") contains major population centers and agricultural regions that depend on limited water resources. The region's precipitation primarily arises from transient equatorward excursions of the Pacific storm track during winter and from the North American monsoon during summer (Seager et al., 2014). Concerningly, global climate models project worsening drought conditions for the region if atmospheric greenhouse gases continue to increase over the 21st century (Cook et al., 2020). Models strongly agree that increased evapotranspiration caused by warming air temperatures will contribute to greater future likelihood of drought conditions in the Southwest (Dai et al., 2018; Williams et al., 2020). However, the severity of future drought conditions in the Southwest will also depend on future changes in precipitation, for which there is much less agreement among models.

Figure 1 illustrates the range of possible 21st century precipitation trends for a single future emissions scenario (Shared Socioeconomic Pathway [SSP] 3–7.0) from the latest generation of global climate models, those from phase 6 of the Coupled Model Intercomparison Project (CMIP6). On average, models indicate increased precipitation in the Southwest in winter (Figure 1b), decreased precipitation in spring (Figure 1f), and trends of inconsistent sign in summer and autumn (Figures 1j and 1n) (see also Cook et al., 2020). The increased precipitation during winter has been attributed to an eastward extension of the subtropical jet stream and Pacific storm track (Neelin et al., 2013), while the decreased precipitation during spring has been attributed to enhanced dry advection by the climatological westerly winds (Ting et al., 2018). Yet, examining only the multi-model mean ignores the huge range of 21st century precipitation trends for the Southwest projected by individual model runs. Compositing the model simulations with the 20% smallest and largest precipitation trends over the Southwest reveals possible drying and wetting scenarios during all seasons (Figure 1, first and third columns). Determining

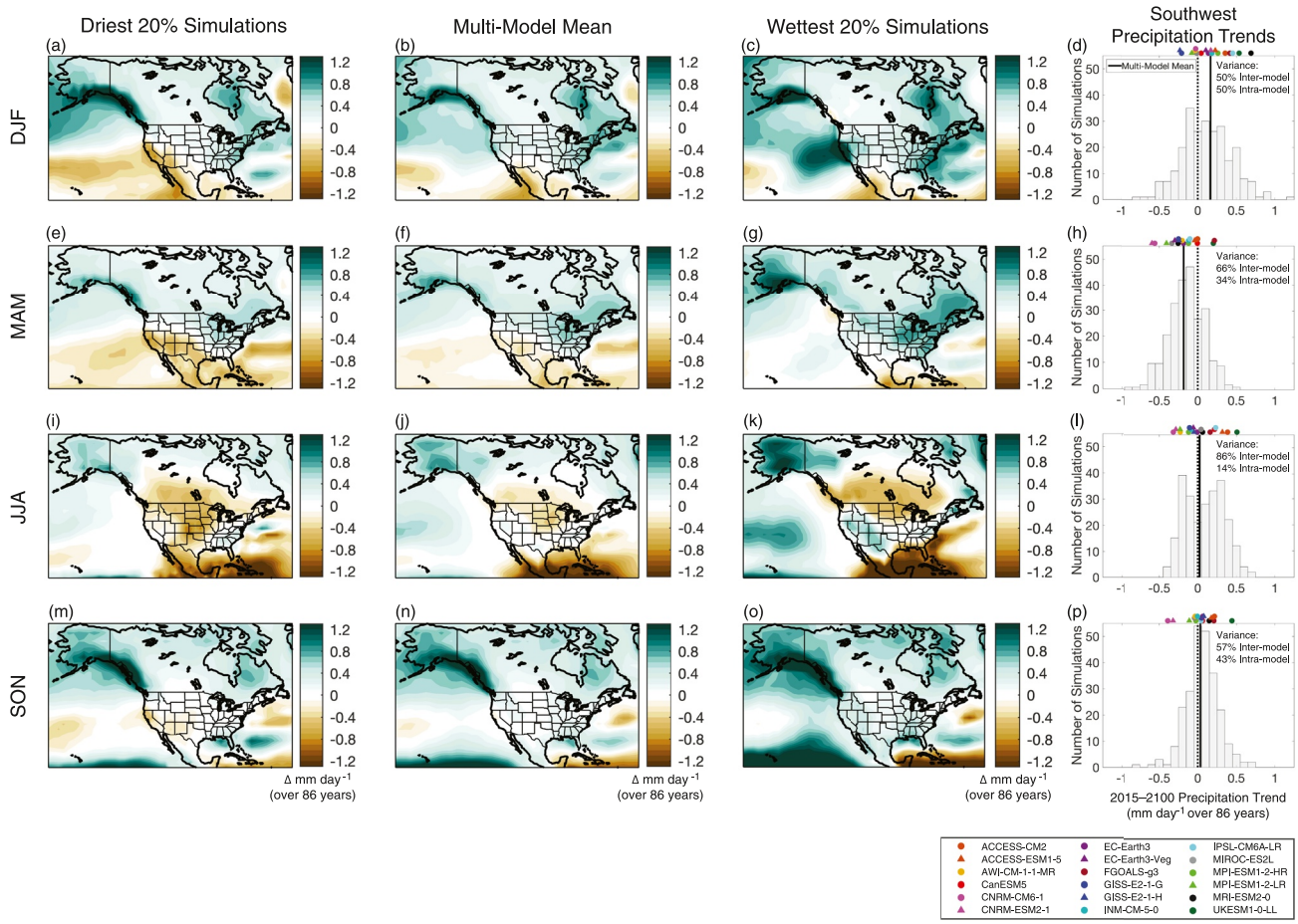

Figure 1. 2015–2100 precipitation trends (mm day^{-1} change over 86 years) for the Shared Socioeconomic Pathway 3-7.0 scenario. Second column: Coupled Model Intercomparison Project Phase 6 multi-model mean. First (third) column: Average of the 20% of simulations with the driest (wettest) trends over the southwestern United States. Fourth column: Histograms of trends for the southwestern United States (vertical black line: multi-model mean; colored symbols: mean trend for all ensemble members of a given model).

whether these scenarios are equally likely is important, as increased precipitation in summer would help to mitigate drought risk (Figure 1k) whereas large decreases in precipitation in winter and spring (Figures 1a and 1e) would exacerbate the risk of drought in a warming climate.

Most previous studies examining the model spread in projected 21st century precipitation trends for the Southwest have focused on winter months, when climatological precipitation is greatest along the California coast. Using CMIP5 models, Neelin et al. (2013) and Langenbrunner et al. (2015) tied variability in wintertime precipitation trends across models to future changes in the position and strength of the Pacific subtropical jet stream and associated storm track, which vary greatly across models (see also Chang et al., 2015; Choi et al., 2016). Similarly, for both CMIP5 and CMIP6 models, Simpson et al. (2016, 2021) related the inter-model spread in future Southwest wintertime precipitation trends to the inter-model spread in the climatological stationary wave field and its response to climate change. Finally, Schmidt and Grise (2021) found that, in CMIP6 models, the largest 21st century wintertime precipitation trends in the Southwest were favored by model simulations with both (a) trends toward an El Niño-like state in the tropical Pacific and (b) trends toward the negative phase of the East Pacific teleconnection pattern, which is similar to the California Precipitation Mode (Chen et al., 2021).

The question remains whether the varying precipitation scenarios depicted in Figure 1 are equally likely due to random internal variability, or whether some scenarios are not as physically plausible as others. The goal of this study is to explore the role of model differences in current and future states of the large-scale atmospheric circulation in contributing to different 21st century precipitation scenarios for the Southwest. While some previous

studies have examined similar issues in CMIP5 models (as noted above), they relied on only a small number of ensemble members that were available for each model, complicating the separation of inter-model differences from internal variability. With a much greater number of ensemble members available from many CMIP6 models, I show here that the models with present-day atmospheric circulations most dissimilar from observations over western North America are the ones that project the most extreme outlier precipitation trends for the Southwest in the future.

2. Data and Methods

The primary data source for this study is global climate model output from CMIP6 (Eyring et al., 2016) for the SSP3-7.0 future emissions scenario (2015–2100), a medium-to-high emissions scenario that reaches a radiative forcing of 7.0 W m^{-2} greater than pre-industrial levels by the year 2100. The SSP3-7.0 scenario is chosen because (a) it was requested to have the largest number of ensemble members per model of any 21st century scenario (O'Neill et al., 2016), (b) it has a higher signal-to-noise ratio than more moderate emissions scenarios, making it easier to discern the climate change signal from internal variability (O'Neill et al., 2016), and (c) the higher SSP5-8.5 emissions scenario has been argued to be implausible (Hausfather & Peters, 2020). For this study, I use all available SSP3-7.0 simulations from models with at least five ensemble members (a total of 248 simulations from 18 models; see list in Table S1 in Supporting Information S1). Furthermore, I have verified that CMIP6 model precipitation trends for the Southwest for the SSP3-7.0 scenario are correlated with and therefore representative of those from other emissions scenarios (Figure S1 in Supporting Information S1).

To assess the validity of models' present-day atmospheric circulations, I also examine the historical runs from CMIP6 models, which are forced by observed 1850–2014 radiative forcings. Models' present-day climatologies are found by merging 2015–2021 values from each SSP3-7.0 simulation with 1992–2014 values from the corresponding parent historical simulation, and then the models' climatologies are compared with observations using two reanalysis products, the fifth generation ECMWF atmospheric reanalysis (ERA5; Hersbach et al., 2020) and the NASA Modern-Era Retrospective analysis for Research and Applications Version 2 (MERRA-2; Gelaro et al., 2017).

I follow Schmidt and Grise (2021) to partition variance across the multi-model ensemble. For example, consider an array of 248 21st century precipitation trends, one from each of the CMIP6 simulations used in this study. If we replace each value in the array by the mean over all ensemble members for that particular model (i.e., the new array will have 18 values that are repeated multiple times corresponding to the number of ensemble members for that model) and correlate it with the original array, the square of the correlation coefficient will be the variance explained by inter-model differences. Likewise, if we subtract the mean for each model from each value in the array and correlate it with the original array, the square of the correlation coefficient will be the variance explained by intra-model differences (internal variability).

3. Results

I begin by reviewing the distribution of 2015–2100 precipitation trends for the Southwest from all 248 CMIP6 simulations used in this study, which are shown in the histograms in Figure 1 (right column). Here, to define the Southwest, precipitation is averaged over California, Nevada, Utah, Arizona, Colorado, and New Mexico. These histograms reveal that most model simulations (72%) project decreasing precipitation in spring, while approximately 60% of simulations project increasing precipitation during other seasons. However, during all seasons, the disparity in the magnitude and sign of the trends is striking. The variance in precipitation trends among simulations is roughly equally distributed between inter-model and intra-model variance in winter but becomes dominated by inter-model differences in warmer months.

I now investigate the role of the large-scale atmospheric circulation in this vast spread of precipitation trends across simulations. To do this, I focus on the 500 hPa geopotential height field with the zonal mean removed (Z^*), which helps to identify the positions of troughs and ridges in the mid-tropospheric flow. Qualitatively similar conclusions can be drawn by examining zonal and meridional wind (Figures S2–S3 in Supporting Information S1).

Figure 2 shows the differences in 21st century (2015–2100) 500 hPa Z^* trends (left column) and the present-day (1992–2021) 500 hPa Z^* climatology (right column) between the 20% of model simulations with the wettest

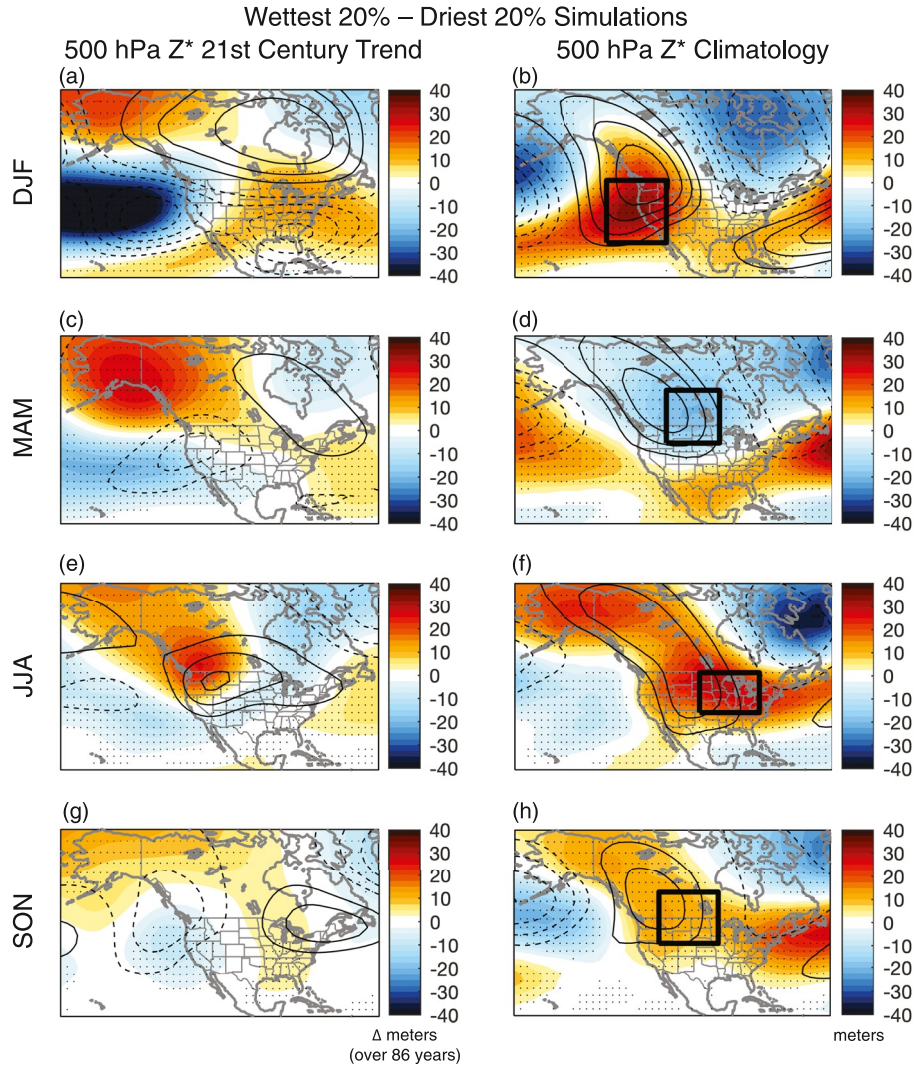

Figure 2. Differences in (left) 2015–2100 500 hPa Z^* trends and (right) 1992–2021 500 hPa Z^* climatology between the 20% of simulations with the wettest and driest 21st century precipitation trends over the southwestern United States (as shown in Figure 1). Thin solid lines indicate multi-model mean (left) trend (contour interval: 5 m change over 86 years) and (right) climatology (contour interval: 20 m), with dashed contours denoting negative values. Stippling indicates differences that are statistically significant ($p < 0.05$) via Student's t-test. Black boxes highlight regions examined in Figure 3.

and driest 21st century precipitation trends for the Southwest. On average, CMIP6 models indicate negative 500 hPa Z^* trends over the eastern North Pacific Ocean in response to SSP3-7.0 forcing (Figure 2, left, dashed contours). During all seasons, model simulations with the largest positive precipitation trends in the Southwest are associated with the largest negative Z^* trends off the western coast of North America (Figure 2, left, shading). During winter and spring, this anomalous cyclonic flow is consistent with an eastward extension and strengthening of the subtropical jet stream (Figure S2 in Supporting Information S1; Neelin et al., 2013), enhancing storm track-driven rainfall along the California coast (Figures 1c and 1g). During summer, the negative Z^* trends over the subtropical eastern North Pacific are associated with a weakening and northward broadening of the North Pacific surface subtropical high-pressure system (not shown), which allows for anomalous eastward moisture transport from the Pacific into the North American monsoon region (Figure S2e in Supporting Information S1; Geil et al., 2013). Accompanying the negative Z^* trends over the Pacific during summer are positive Z^* trends over western North America (Figure 2e, solid contours). These trends represent an expansion and westward extension of the summertime mid-tropospheric climatological ridge over North America in a warming climate (Pascale et al., 2018), creating anomalous easterly flow from the Great Plains (Figure S2e in Support-

ing Information S1) that promotes more precipitation in the interior western United States (Figure 1k; Liang & Zhang, 2022). Finally, during autumn, the negative Z^* trends along the west coast of North America indicate the development of an anomalous mid-tropospheric trough over the 21st century that extends further southward in the wettest simulations (Figure 2g), leading to more precipitation in the Southwest (Figure 1o).

The spread in the future trends in the atmospheric circulation across simulations is determined, at least in part, by intra-model variance rather than by differences in the forced circulation response among models (Figure S4 in Supporting Information S1). Thus, inherently unpredictable internal variability in the atmospheric circulation can lead to vastly different future precipitation scenarios for the Southwest (Deser et al., 2012). However, as Figure 2 (right column) shows, 21st century precipitation trends over the Southwest are also closely linked to the representation of the present-day atmospheric circulation in CMIP6 models, and this variance is almost entirely driven by inter-model differences (Figure S4 in Supporting Information S1).

The present-day mid-tropospheric flow is characterized by a ridge over the west coast of North America, which migrates toward the interior of the continent during warmer months (Figure 2, right, solid contours). On average, CMIP6 models underestimate the observed strength of this ridge during winter and overestimate its strength during other seasons (Figure S5 in Supporting Information S1), but the representation of the large-scale flow over western North America varies greatly by model. During all seasons, the strength of the southern flank of a model's present-day climatological ridge is closely related to its projected 21st century precipitation trends for the Southwest (Figure 2, right, shading). To better understand this relationship, in Figure 3, I examine scatter plots between 21st century precipitation trends for the Southwest and the 500 hPa Z^* climatology within the boxed regions in Figure 2 (right). The boxes outline the regions of the largest correlations (not shown), but the results are not sensitive to their specific definition.

During winter, model simulations with a stronger present-day climatological ridge over the west coast of the United States generally have the largest 21st century precipitation trends in the Southwest ($r = 0.45$; Figure 3a). This relationship is largely driven by two models from one modeling center (NASA GISS), as the correlation reduces to $r = 0.24$ without these models. The climatological ridge off the California coast is virtually absent in the GISS models, permitting the strongest climatological jet stream in this region among the CMIP6 models examined (as was noted by Neelin et al., 2013 for the CMIP5 version of the GISS model). As a result, the GISS models have among the greatest climatological wintertime precipitation in the Southwest (Figure S6a in Supporting Information S1). With climate change, negative 500 hPa Z^* trends over the eastern Pacific and western North America (Figure 2a) allow the subtropical jet stream and associated storm track precipitation to extend closer to the Southwest in most models. But in the GISS models, the subtropical jet is already well established in the region in the present-day climatology and is thus shifted further southward with climate change, reducing future storm track-driven precipitation in the region.

During spring, model simulations with a stronger present-day climatological ridge over the northern Great Plains generally have the driest 21st century precipitation trends in the Southwest ($r = -0.53$; Figure 3b). These models also tend to have a stronger climatological trough in the central North Pacific (Figure 2d), corresponding to a more positive Pacific-North America pattern (PNA)-like Rossby wave train in the climatology. Such a flow configuration during spring is associated with a split-flow regime with a southerly subtropical jet stream and storm track directed into the Southwest (Leathers et al., 1991), promoting more climatological precipitation in the current climate (Figure S6b in Supporting Information S1) and thus greater potential for drying over the 21st century, such as via the mechanism of Ting et al. (2018).

During summer, model simulations with a stronger present-day climatological ridge over the midwestern United States generally have the wettest 21st century precipitation trends in the Southwest ($r = 0.71$; Figure 3c). The stronger climatological ridge is associated with weaker westerly flow across the southern United States (Figure S2f in Supporting Information S1) and stronger low-level southerly flow over the Great Plains (Figure S3f in Supporting Information S1). Consequently, relative to other models, there is anomalous southeasterly flow from the moisture rich southern Great Plains into the Southwest in these models. All else being equal, with increasing global temperatures, increased moisture advection by the climatological flow would promote enhanced summertime precipitation in the Southwest in these models by the end of the 21st century.

Finally, during autumn, model simulations with a stronger present-day climatological ridge over the northern Great Plains generally have the wettest 21st century precipitation trends in the Southwest ($r = 0.39$; Figure 3d).

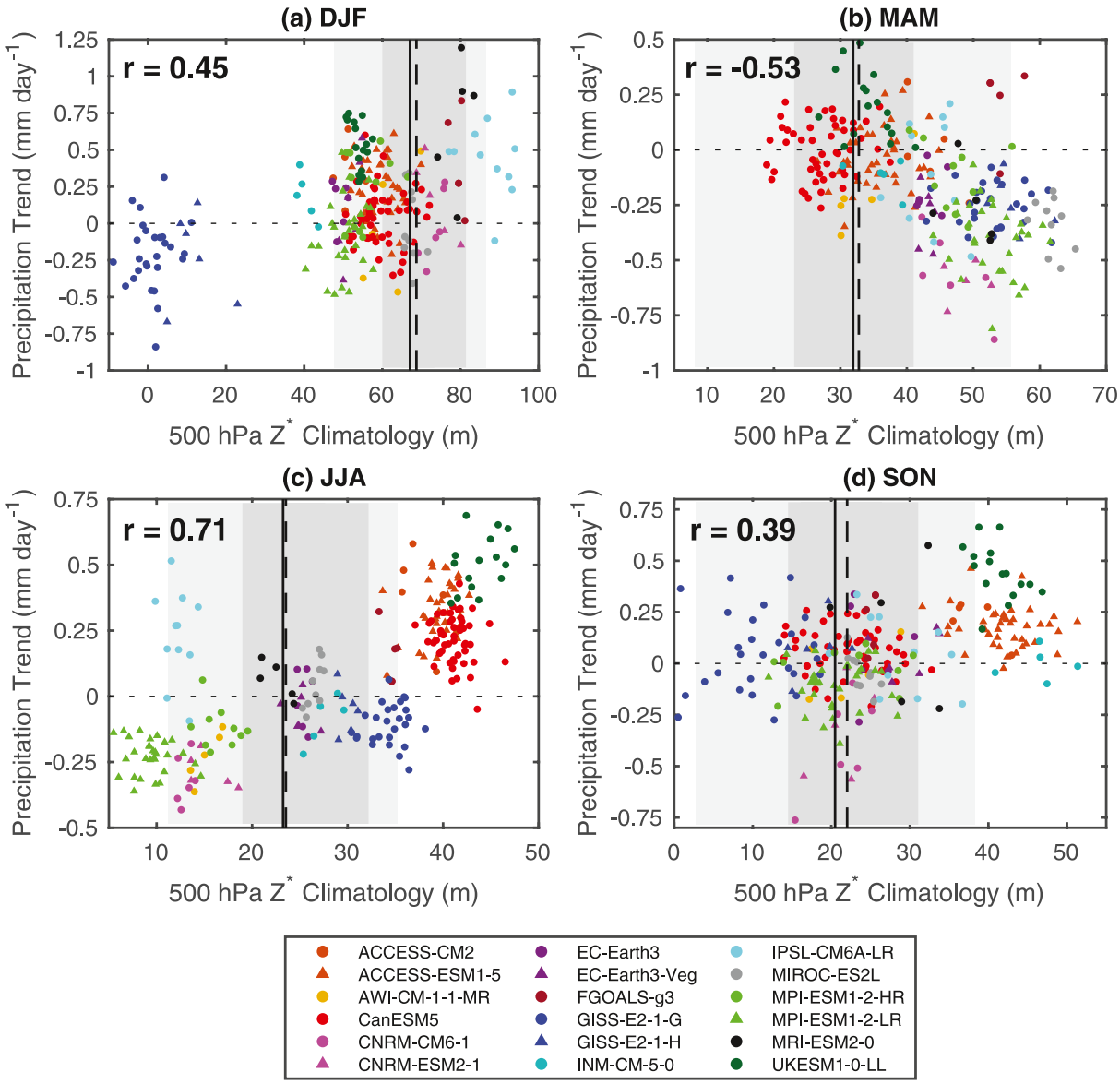

Figure 3. Scatter plots between 1992 and 2021 500 hPa Z^* climatology within the boxed regions shown in Figure 2 and 2015–2100 projected precipitation trends over the southwestern United States (units: mm day^{-1} change over 86 years) for 248 Coupled Model Intercomparison Project Phase 6 simulations. Solid (dashed) vertical line: 1992–2021 500 hPa Z^* climatology from ERA5 (MERRA-2) reanalysis. Light shading: One standard deviation bounds on ERA5 mean. Dark shading: Range spanning 95% confidence bounds on means of 1000 random 30-year samples (with replacement) from ERA5 for both the 1959–2021 and 1992–2021 periods.

This relationship is the weakest among the four seasons and is even weaker if the UKESM1-0-LL model is excluded (r = 0.28). Like the springtime relationship discussed above (Figure 3b), models with a stronger present-day climatological ridge over the northern Great Plains also tend to have a stronger climatological trough in the central North Pacific (Figure 2h), corresponding to a more positive PNA-like Rossby wave train in the climatology. However, in contrast to spring, this flow configuration during autumn is associated with a more poleward Pacific jet stream, deflecting storm track precipitation northward of the western continental United States (Leathers et al., 1991). Because of the seasonal climatology of the Pacific jet streams, a positive PNA-like flow bias would act to enhance climatological precipitation in the Southwest during spring and suppress it during autumn, explaining the oppositely signed spring and autumn relationships in Figure 3. So, models with the strongest climatological ridges over western North America during autumn have the potential for the greatest precipitation increases over the 21st century if the ridge were to weaken with climate change (Figure 2g).

In summary, Figures 2 and 3 clearly demonstrate distinct seasonal relationships between the strength of a model's present-day climatological ridge over western North America and its projected 21st century precipitation trends for the Southwest, and as argued above, there are dynamically consistent explanations for these relationships during each season. Because the strength of the present-day climatological ridge is known to good approximation from reanalyses, I can therefore estimate which models may have more plausible future precipitation scenarios for the Southwest. To do this, I have plotted the 1992–2021 500 hPa Z^* climatology from two reanalyses, ERA5 (solid vertical line) and MERRA-2 (dashed vertical line), on Figure 3. As a measure of uncertainty, I also show the ±1 standard deviation range about the ERA5 mean (light gray) and the range spanning the 95% confidence bounds on the mean of 1000 random 30-year samples (with replacement) from ERA5 for both the 1959–2021 and 1992–2021 periods (dark gray).

The results reveal that models with very weak climatological ridges along the Pacific coast during winter (Figure 3a) and very strong climatological ridges over western North America during other seasons (Figures 3b–3d) have present-day atmospheric circulations over North America that are inconsistent with observations. Because of the dynamical linkages of the present-day atmospheric circulation with future precipitation trends discussed above, we should be skeptical about the physical plausibility of future precipitation scenarios projected by these models, which show some of the largest drying trends during winter and spring and some of the largest wetting trends during summer and autumn (see points outside of gray shading in Figure 3). Note that it is difficult to conclusively evaluate whether the relationships in Figure 3 hold in previous generations of models, given the limited number of ensemble members available from those models. Nonetheless, there is some evidence that the summertime relationship (Figure 3c) also exists in CMIP5 models (Figure S7 in Supporting Information S1). Furthermore, recent studies applying machine learning have concluded that future wintertime drying trends for the Southwest are unlikely (Langenbrunner & Neelin, 2017; Li et al., 2022).

To review the key results, Figure 4 shows maps and histograms of the precipitation trends from all models versus those models that fall within the observed circulation constraints from Figure 3. Here, a model is considered to fall within the observational constraints if the 95% confidence bounds on its 500 hPa Z^* climatology (determined using 1000 random 30-year samples with replacement from the first ensemble member of each model) overlap the gray shading in Figure 3. Taking these observational constraints into account, approximately 65%–75% of the remaining simulations show increased 21st century precipitation in the Southwest during winter and decreased 21st century precipitation during spring and summer. The observational constraint is particularly noteworthy in summer, as more simulations show increased precipitation without any observational constraint. For autumn, the observational constraint does little to increase confidence in the expected sign of the precipitation response, as roughly equal numbers of the remaining simulations show wetting and drying trends.

4. Conclusions

An accurate understanding of potential future precipitation changes is vital for the water-limited region of the southwestern United States. Yet, CMIP6 global climate models project vastly different 21st century precipitation trends for the region, even if forced by identical anthropogenic emissions (Figure 1). In this study, I have explored the role of model differences in the current and future states of the large-scale atmospheric circulation in contributing to different 21st century precipitation scenarios for the Southwest. Future precipitation trends in the Southwest are closely linked to the development of an anomalous mid-tropospheric trough off the west coast of North America over the 21st century (Figure 2, left), which depends at least in part on future unpredictable internal variability. However, future precipitation trends in the Southwest are also closely linked to models' representation of the present-day mid-tropospheric ridge over western North America (Figure 2, right). Models whose present-day mid-tropospheric flow differs most from observations are responsible for the most extreme outlier precipitation trends for the Southwest over the 21st century, casting doubt on the physical plausibility of future scenarios with large drying during winter and large wetting during summer (Figures 3 and 4).

Because they are supported by plausible dynamical arguments (see Section 3), the relationships found in the scatter plots in Figure 3 do not appear to occur by chance, suggesting that improper mid-tropospheric flow over western North America biases a model's ability to make realistic 21st century precipitation projections for the Southwest. Investigating the origin of the models' present-day atmospheric circulation biases over North America should be an important focus for future studies. Johnson et al. (2020) linked models' climatological biases

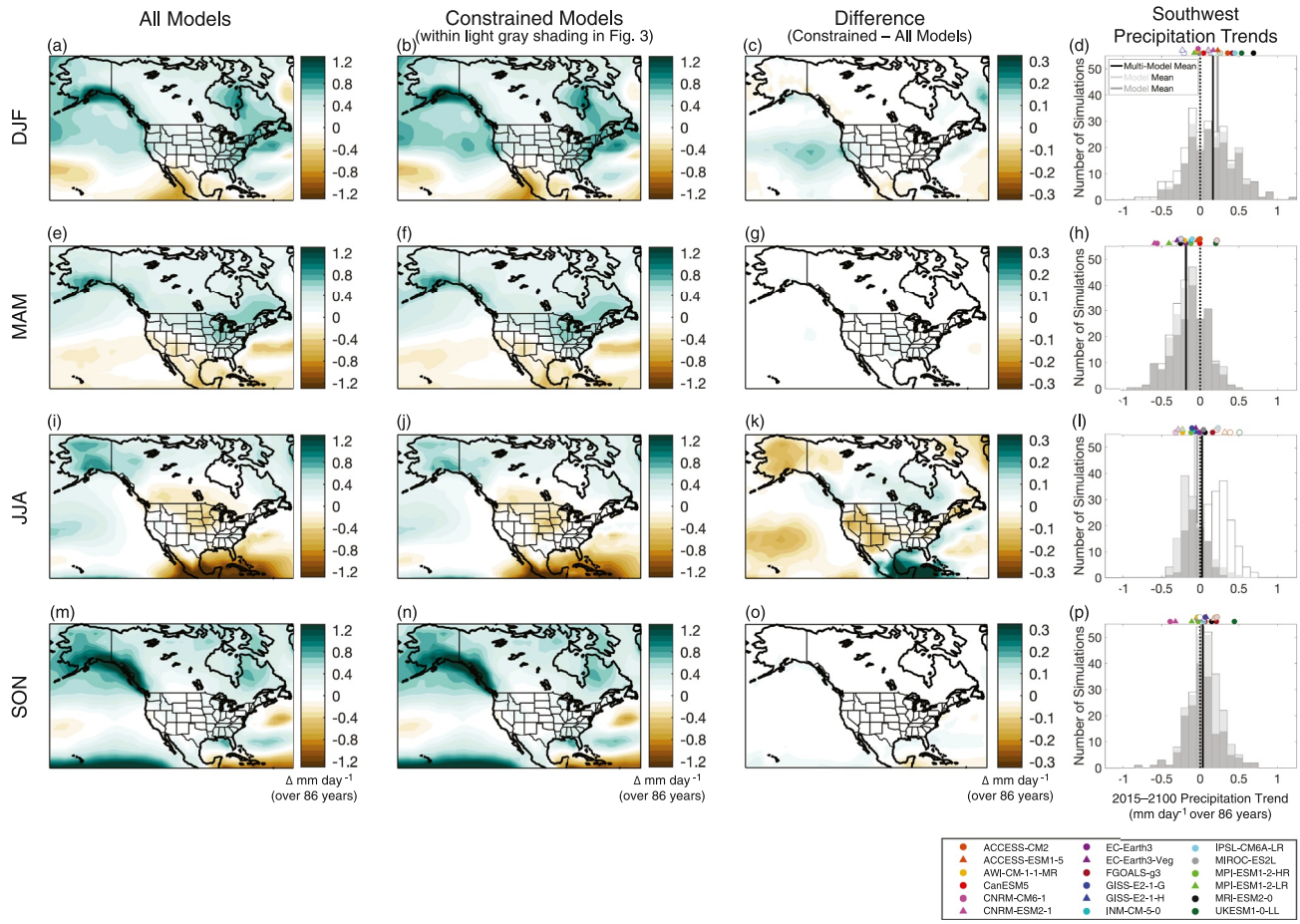

Figure 4. As in Figure 1, but for 2015–2100 precipitation trends from (first column) Coupled Model Intercomparison Project Phase 6 multi-model mean, (second column) mean from models falling within the observational constraints from Figure 3 (see text for details), and (third column) difference. Fourth column: Histograms from Figure 1 shown in white, with light and dark shading highlighting simulations from models falling within the corresponding shading in Figure 3. Model symbols are filled in white for models falling outside the observational constraints and gray (colors) for models falling within the light (dark) gray shading in Figure 3.

in tropical Atlantic and Pacific sea surface temperatures (SSTs) with their representation of the climatological circulation and precipitation over North America. Similarly, biases in trends in tropical Pacific SSTs influence the representation of North American circulation and precipitation trends in models (Lehner et al., 2018; Seager et al., 2019).

It is important to acknowledge that there are a vast array of other processes that are also relevant for a model's fidelity in simulating precipitation in the Southwest, including but not limited to land surface processes, cloud and precipitation parameterizations, and model representation of topography and other local-scale features. Although biases in these processes will also directly impact 21st century precipitation trends in models, I argue here that an accurate simulation of the present-day large-scale atmospheric circulation over western North America during all four seasons is a necessary (but likely not a sufficient) condition for a model to produce plausible 21st century precipitation projections for the Southwest (see also Maraun et al., 2017).

Data Availability Statement

All data used in this study are freely and publicly available via DOI links provided in the references section: CMIP6 (model references in Table S1 in Supporting Information S1), ERA5 (Hersbach et al., 2019), and MERRA-2 (GMAO, 2015).

Acknowledgments
This study was supported by NOAA's Climate Program Office's Modeling, Analysis, Predictions, and Projections program (grants NA19OAR4310293 and NA21OAR4310476). I acknowledge the World Climate Research Programme, which coordinated and promoted CMIP6, and thank the climate modeling groups for producing and making available their model output, the Earth System Grid Federation (ESGF) for archiving the data and providing access, and the multiple funding agencies who support CMIP6 and ESGF. I thank two anonymous reviewers for helpful comments.

References

Chang, E. K. M., Zheng, C., Lanigan, P., Yau, A. M. W., & Neelin, J. D. (2015). Significant modulation of variability and projected change in California winter precipitation by extratropical cyclone activity. *Geophysical Research Letters*, *42*(14), 5983–5991. https://doi.org/10.1002/2015GL064424

Chen, D., Norris, J., Goldenson, N., Thackeray, C., & Hall, A. (2021). A distinct atmospheric mode for California precipitation. *Journal of Geophysical Research: Atmospheres*, *126*(12), e2020JD034403. https://doi.org/10.1029/2020JD034403

Choi, J., Lu, J., Son, S.-W., Frierson, D. M. W., & Yoon, J.-H. (2016). Uncertainty in future projections of the North Pacific subtropical high and its implication for California winter precipitation change. *Journal of Geophysical Research: Atmospheres*, *121*(2), 795–806. https://doi.org/10.1002/2015JD023858

Cook, B. I., Mankin, J. S., Marvel, K., Williams, A. P., Smerdon, J. E., & Anchukaitis, K. J. (2020). Twenty-first century drought projections in the CMIP6 forcing scenarios. *Earth's Future*, *8*, e2019EF001461. https://doi.org/10.1029/2019EF001461

Dai, A., Zhao, T., & Chen, J. (2018). Climate change and drought: A precipitation and evaporation perspective. *Current Climate Change Reports*, *4*(3), 301–312. https://doi.org/10.1007/s40641-018-0101-6

Deser, C., Knutti, R., Solomon, S., & Phillips, A. S. (2012). Communication of the role of natural variability in future North American climate. *Nature Climate Change*, *2*(11), 775–779. https://doi.org/10.1038/nclimate1562

Eyring, V., Bony, S., Meehl, G. A., Senior, C. A., Stevens, B., Stouffer, R. J., & Taylor, K. E. (2016). Overview of the Coupled Model Intercomparison Project phase 6 (CMIP6) experimental design and organization. *Geoscientific Model Development*, *9*(5), 1937–1958. https://doi.org/10.5194/gmd-9-1937-2016

Geil, K. L., Serra, Y. L., & Zeng, X. (2013). Assessment of CMIP5 model simulations of the North American monsoon system. *Journal of Climate*, *26*(22), 8787–8801. https://doi.org/10.1175/JCLI-D-13-00044.1

Gelaro, R., McCarty, W., Suárez, M. J., Todling, R., Molod, A., Takacs, L., et al. (2017). The Modern-Era Retrospective analysis for Research and Applications, version 2 (MERRA-2). *Journal of Climate*, *30*(14), 5419–5454. https://doi.org/10.1175/JCLI-D-16-0758.1

Global Modeling and Assimilation Office (GMAO). (2015). MERRA-2 instM_3d_ana_Np: 3d, monthly mean, instantaneous, pressure-level, analysis, analyzed meteorological fields V5.12.4 [Dataset]. Goddard Earth Sciences Data and Information Services Center (GES DISC). https://doi.org/10.5067/V92O8XZ30XBI

Hausfather, Z., & Peters, G. P. (2020). Emissions—The 'business as usual' story is misleading. *Nature*, *577*, 618–620. https://doi.org/10.1038/d41586-020-00177-3

Hersbach, H., Bell, B., Berrisford, P., Biavati, G., Horányi, A., Muñoz Sabater, J., et al. (2019). ERA5 monthly averaged data on pressure levels from 1979 to present[Dataset]. Chang. https://doi.org/10.24381/cds.6860a573

Hersbach, H., Bell, B., Berrisford, P., Hirahara, S., Horányi, A., Muñoz-Sabater, J., et al. (2020). The ERA5 global reanalysis. *Quarterly Journal of the Royal Meteorological Society*, *146*(730), 1999–2049. https://doi.org/10.1002/qj.3803

Johnson, N. C., Krishnamurthy, L., Wittenberg, A. T., Xiang, B., Vecchi, G. A., Kapnick, S. B., & Pascale, S. (2020). The impact of sea surface temperature biases on North American precipitation in a high-resolution climate model. *Journal of Climate*, *33*(6), 2427–2447. https://doi.org/10.1175/JCLI-D-19-0417.1

Langenbrunner, B., & Neelin, J. D. (2017). Pareto-optimal estimates of California precipitation change. *Geophysical Research Letters*, *44*, 12436–12446. https://doi.org/10.1002/2017GL075226

Langenbrunner, B., Neelin, J. D., Lintner, B. R., & Anderson, B. T. (2015). Patterns of precipitation change and climatological uncertainty among CMIP5 models, with a focus on the midlatitude Pacific storm track. *Journal of Climate*, *28*(19), 7857–7872. https://doi.org/10.1175/JCLI-D-14-00800.1

Leathers, D. J., Yarnal, B., & Palecki, M. A. (1991). The Pacific/North American teleconnection pattern and United States climate. Part I: Regional temperature and precipitation associations. *Journal of Climate*, *4*(5), 517–528. https://doi.org/10.1175/1520-0442(1991)004%3C0517:TPATPA%3E2.0.CO;2

Lehner, F., Deser, C., Simpson, I. R., & Terray, L. (2018). Attributing the U.S. Southwest's recent shift into drier conditions. *Geophysical Research Letters*, *45*(12), 6251–6261. https://doi.org/10.1029/2018GL078312

Li, F., Zhu, Q., Riley, W. J., Yuan, K., Wu, H., & Gui, Z. (2022). Wetter California projected by CMIP6 models with observational constraints under a high GHG emission scenario. *Earth's Future*, *10*(4), e2022EF002694. https://doi.org/10.1029/2022EF002694

Liang, W., & Zhang, M. (2022). Increasing future precipitation in the southwestern US in the summer and its contrasting mechanism with decreasing precipitation in the spring. *Geophysical Research Letters*, *49*(2), e2021GL096283. https://doi.org/10.1029/2021GL096283

Maraun, D., Shepherd, T. G., Widmann, M., Zappa, G., Walton, D., Gutierrez, J. M., et al. (2017). Towards process-informed bias correction of climate change simulations. *Nature Climate Change*, *7*(11), 764–773. https://doi.org/10.1038/nclimate3418

Neelin, J. D., Langenbrunner, B., Meyerson, J. E., Hall, A., & Berg, N. (2013). California winter precipitation change under global warming in the Coupled Model Intercomparison Project phase 5 ensemble. *Journal of Climate*, *26*(17), 6238–6256. https://doi.org/10.1175/JCLI-D-12-00514.1

O'Neill, B. C., Tebaldi, C., van Vuuren, D. P., Eyring, V., Friedlingstein, P., Hurtt, G., et al. (2016). The Scenario Model Intercomparison Project (ScenarioMIP) for CMIP6. *Geoscientific Model Development*, *9*, 3461–3482. https://doi.org/10.5194/gmd-9-3461-2016

Pascale, S., Kapnick, S. B., Bordoni, S., & Delworth, T. L. (2018). The influence of CO_2 forcing on North American monsoon moisture surges. *Journal of Climate*, *31*(19), 7949–7968. https://doi.org/10.1175/JCLI-D-18-0007.1

Schmidt, D. F., & Grise, K. M. (2021). Drivers of twenty-first-century U.S. winter precipitation trends in CMIP6 models: A storyline-based approach. *Journal of Climate*, *34*(16), 6875–6889. https://doi.org/10.1175/JCLI-D-21-0080.1

Seager, R., Cane, M., Henderson, N., Lee, D.-E., Abernathey, R., & Zhang, H. (2019). Strengthening tropical Pacific zonal sea surface temperature gradient consistent with rising greenhouse gases. *Nature Climate Change*, *9*, 517–522. https://doi.org/10.1038/s41558-019-0505-x

Seager, R., Neelin, D., Simpson, I., Liu, H., Henderson, N., Shaw, T., et al. (2014). Dynamical and thermodynamical causes of large-scale changes in the hydrological cycle over North America in response to global warming. *Journal of Climate*, *27*(20), 7921–7948. https://doi.org/10.1175/JCLI-D-14-00153.1

Simpson, I. R., McKinnon, K. A., Davenport, F. V., Tingley, M., Lehner, F., Al Fahad, A., & Chen, D. (2021). Emergent constraints on the large-scale atmospheric circulation and regional hydroclimate: Do they still work in CMIP6 and how much can they actually constrain the future? *Journal of Climate*, *34*(15), 6355–6377. https://doi.org/10.1175/JCLI-D-21-0055.1

Simpson, I. R., Seager, R., Ting, M., & Shaw, T. A. (2016). Causes of change in Northern Hemisphere winter meridional winds and regional hydroclimate. *Nature Climate Change*, *6*(1), 65–70. https://doi.org/10.1038/nclimate2783

Ting, M., Seager, R., Li, C., Liu, H., & Henderson, N. (2018). Mechanism of future spring drying in the southwestern United States in CMIP5 models. *Journal of Climate*, *31*(11), 4265–4279. https://doi.org/10.1175/JCLI-D-17-0574.1

Williams, A. P., Cook, E. R., Smerdon, J. E., Cook, B. I., Abatzoglou, J. T., Bolles, K., et al. (2020). Large contribution from anthropogenic warming to an emerging North American megadrought. *Science*, *368*(6488), 314–318. https://doi.org/10.1126/science.aaz9600

References From the Supporting Information

Adler, R. F., Huffman, G. J., Chang, A., Ferraro, R., Xie, P., Janowiak, J., et al. (2003). The version-2 Global Precipitation Climatology Project (GPCP) monthly precipitation analysis (1979–present). *Journal of Hydrometeorology*, *4*(6), 1147–1167. https://doi.org/10.1175/1525-7541(2003)004%3C1147:TVGPCP%3E2.0.CO;2

Boucher, O., Denvil, S., Levavasseur, G., Cozic, A., Caubel, A., Foujols, M.-A., et al. (2019). IPSL IPSL-CM6A-LR model output prepared for CMIP6 ScenarioMIP [Dataset]. Earth System Grid Federation. https://doi.org/10.22033/ESGF/CMIP6.1532

Dix, M., Bi, D., Dobrohotoff, P., Fiedler, R., Harman, I., Law, R., et al. (2019). CSIRO- ARCCSS ACCESS-CM2 model output prepared for CMIP6 ScenarioMIP [Dataset]. Earth System Grid Federation. https://doi.org/10.22033/ESGF/CMIP6.2285

EC-Earth Consortium (EC-Earth). (2019). EC-Earth-Consortium EC-Earth3-Veg model output prepared for CMIP6 ScenarioMIP [Dataset]. Earth System Grid Federation. https://doi.org/10.22033/ESGF/CMIP6.727

Good, P., Sellar, A., Tang, Y., Rumbold, S., Ellis, R., Kelley, D., et al. (2019). MOHC UKESM1.0-LL model output prepared for CMIP6 ScenarioMIP [Dataset]. Earth System Grid Federation. https://doi.org/10.22033/ESGF/CMIP6.1567

Li, L. (2019). CAS FGOALS-g3 model output prepared for CMIP6 ScenarioMIP [Dataset]. Earth System Grid Federation. https://doi.org/10.22033/ESGF/CMIP6.2056

NASA Goddard Institute for Space Studies (NASA/GISS). (2020). NASA-GISS GISS-E2.1H model output prepared for CMIP6 ScenarioMIP[Dataset]. Earth System Grid Federation. https://doi.org/10.22033/ESGF/CMIP6.2080

Schupfner, M., Wieners, K.-H., Wachsmann, F., Steger, C., Bittner, M., Jungclaus, J., et al. (2019). DKRZ MPI-ESM1.2-HR model output prepared for CMIP6 ScenarioMIP [Dataset]. Earth System Grid Federation. https://doi.org/10.22033/ESGF/CMIP6.2450

Seferian, R. (2019). CNRM-CERFACS CNRM-ESM2-1 model output prepared for CMIP6 ScenarioMIP [Dataset]. Earth System Grid Federation. https://doi.org/10.22033/ESGF/CMIP6.1395

Semmler, T., Danilov, S., Rackow, T., Sidorenko, D., Barbi, D., Hegewald, J., et al. (2019). AWI, AWI-CM1.1MR model output prepared for CMIP6 ScenarioMIP [Dataset]. Earth System Grid Federation. https://doi.org/10.22033/ESGF/CMIP6.376

Swart, N. C., Cole, J. N. S., Kharin, V. V., Lazare, M., Scinocca, J. F., Gillett, N. P., et al. (2019). CCCma CanESM5 model output prepared for CMIP6 ScenarioMIP [Dataset]. Earth System Grid Federation. https://doi.org/10.22033/ESGF/CMIP6.1317

Tachiiri, K., Abe, M., Hajima, T., Arakawa, O., Suzuki, T., Komuro, Y., et al. (2019). MIROC MIROC-ES2L model output prepared for CMIP6 ScenarioMIP [Dataset]. Earth System Grid Federation. https://doi.org/10.22033/ESGF/CMIP6.936

Taylor, K. E., Stouffer, R. J., & Meehl, G. A. (2012). An overview of CMIP5 and the experiment design. *Bulletin of the American Meteorological Society*, *93*(4), 485–498. https://doi.org/10.1175/BAMS-D-11-00094.1

Voldoire, A. (2019). CNRM-CERFACS CNRM-CM6-1 model output prepared for CMIP6 ScenarioMIP [Dataset]. Earth System Grid Federation. https://doi.org/10.22033/ESGF/CMIP6.1384

Volodin, E., Mortikov, E., Gritsun, A., Lykossov, V., Galin, V., Diansky, N., et al. (2019). INM INM-CM5-0 model output prepared for CMIP6 ScenarioMIP [Dataset]. Earth System Grid Federation. https://doi.org/10.22033/ESGF/CMIP6.12322

Wieners, K.-H., Giorgetta, M., Jungclaus, J., Reick, C., Esch, M., Bittner, M., et al. (2019). MPI-M MPIESM1.2-LR model output prepared for CMIP6 ScenarioMIP [Dataset]. Earth System Grid Federation. https://doi.org/10.22033/ESGF/CMIP6.793

Xie, P., & Arkin, P. A. (1997). Global precipitation: A 17-year monthly analysis based on gauge observations, satellite estimates, and numerical model outputs. *Bulletin of the American Meteorological Society*, *78*(11), 2539–2558. https://doi.org/10.1175/1520-0477(1997)078%3C2539:GPAYMA%3E2.0.CO;2

Yukimoto, S., Koshiro, T., Kawai, H., Oshima, N., Yoshida, K., Urakawa, S., et al. (2019). MRI MRI-ESM2.0 model output prepared for CMIP6 ScenarioMIP [Dataset]. Earth System Grid Federation. https://doi.org/10.22033/ESGF/CMIP6.638

Ziehn, T., Chamberlain, M., Lenton, A., Law, R., Bodman, R., Dix, M., et al. (2019). CSIRO ACCESS-ESM1.5 model output prepared for CMIP6 ScenarioMIP [Dataset]. Earth System Grid Federation. https://doi.org/10.22033/ESGF/CMIP6.2291